View Online / Journal Homepage / Table of Contents for this issue

Organic & Biomolecular Chemistry

This article is part of the

OBC 10th anniversary

themed issue

All articles in this issue will be gathered together online at

www.rsc.org/OBC10

Downloaded by University of California - San Diego on 01 September 2012
Published on 14 May 2012 on http://pubs.rsc.org | doi:10.1039/C2OB25200G

Organic & Biomolecular Chemistry

Dynamic Article Links
View Online

Cite this: *Org. Biomol. Chem.*, 2012, **10**, 6094

www.rsc.org/obc

PAPER

[2]Pseudorotaxanes, [2]rotaxanes and metal–organic rotaxane frameworks containing tetra-substituted dibenzo[24]crown-8 wheels†‡

Darren J. Mercer, Joe Yacoub, Kelong Zhu, Stephanie K. Loeb and Stephen J. Loeb*

Received 26th January 2012, Accepted 3rd April 2012
DOI: 10.1039/c2ob25200g

Published on 14 May 2012 on http://pubs.rsc.org | doi:10.1039/C2OB25200G
Downloaded by University of California - San Diego on 01 September 2012

[2]Pseudorotaxanes, [2]rotaxanes and metal–organic rotaxane framework materials that utilise **DB24C8** as the wheel component are well known and structural variations based on changing the axle component are common. Studies in which the **DB24C8** wheel is structurally modified are much more limited. Herein, is described the synthesis of symmetrical **DB24C8** analogues containing four CH_2OR (R = $CH_2CH_2CH_3$, $CH_2(C_6H_5)$, C_6H_5 and C_6H_4(4-COOEt)) substituents on the 4 and 5 positions of the aromatic rings. The effect of these molecular appendages on the stability and structures of the interpenetrated and interlocked molecules derived from these new wheels is described. The major effects are an increase in association constants for the formation of [2]pseudorotaxanes relative to **DB24C8**, the crystal packing of [2]rotaxanes and a change on the internal structure of a 2D MORF (R = C_6H_5) compared to **DB24C8**.

Introduction

The formation of interpenetrated pseudorotaxane molecules involves the molecular recognition, *via* non-covalent interactions, between a linear "axle" and a macrocyclic "wheel".[1] One of the most commonly employed wheels for the formation of these unique chemical species is the macrocyclic polyether dibenzo[24]crown-8 (**DB24C8**).[2] **DB24C8** is a good hydrogen bond acceptor and it was demonstrated early on that the internal diameter and flexibility of this particular crown size was suitable for the threading of simple aromatics guests.[2l] The presence of two electron-rich catechol rings also endows **DB24C8** with a penchant for π-stacking with many of the electron poor axles used in these template pairings.[2]

Most detailed studies on [2]pseudorotaxane formation utilising **DB24C8** have focussed on varying the structural nature of the axle, while variations in the structure of the macrocyclic wheel are much more limited. There are two ways to vary the structure of the **DB24C8** wheel in these systems without changing the essential donor array and ring size. One is to change the nature of the aromatic ring and it has been established that other 24-membered crown ethers such as [24]crown-8 (**24C8**),[3] benzo[24]crown-8 (**B24C8**),[4] naphtho[24]crown-8 (**N24C8**),[5] benzonaphtho[24]crown-8 (**BN24C8**)[6] and dinaphtho[24]crown-8 (**DN24C8**)[7] are capable of forming interpenetrated structures very similar to **DB24C8**. The other way would be to simply add substituents to the existing aromatic rings of **DB24C8**. Although this seems straightforward there are a number of problems. To add a single substituent to only one of the aromatic rings of **DB24C8** requires incorporating the substituent prior to ring formation and a tedious stepwise building up of the 24-membered ring.[8] Achieving mono-substitution on each of the aromatic rings is much more straightforward since **DB24C8** can be used directly as the starting material, but this produces *syn* and *anti* isomers that are often difficult to separate and yield [2]pseudorotaxanes with different association constants; *i.e.* mixtures cannot be used.[9]

In this article, we outline a simple two step methodology for adding flexible CH_2OR groups of various sizes to the 4- and 5-positions of each of the two aromatic rings of **DB24C8**, resulting in new symmetrical, tetra-substituted versions of **DB24C8**.[10] The effect of these substituents on the formation constants and structure of [2]pseudorotaxanes involving a series of 1,2-bis(pyridinium)ethane axles is investigated along with conversion into permanently interlocked [2]rotaxanes. To explore applications; (1) a [2]rotaxane ligand incorporating one of the new crown ether wheels was prepared and coordinated to Ru(II) – the structures of the ligand and complex are described and (2) the effect of including a tetra-substituted wheel into the internal structure of a metal–organic rotaxane framework (MORF)[11] is also reported.

Results and discussion

Crown ether synthesis

The initial tetra-functionalization of **DB24C8** was accomplished utilising a modified version of a preparation involving

Department of Chemistry and Biochemistry, University of Windsor, Windsor, Ontario, Canada, N9B 3P4. E-mail: loeb@uwindsor.ca; Fax: +1 519 973 7098; Tel: +1 519 253 3000

†Electronic supplementary information (ESI) available: ^1H and ^{13}C NMR spectra for all crown ethers and [2]rotaxanes. CCDC 864507–864513. For ESI and crystallographic data in CIF or other electronic format see DOI: 10.1039/c2ob25200g

‡This article is part of the *Organic & Biomolecular Chemistry* 10th Anniversary issue.

This journal is © The Royal Society of Chemistry 2012

View Online

Downloaded by University of California - San Diego on 01 September 2012
Published on 14 May 2012 on http://pubs.rsc.org | doi:10.1039/C2OB25200G

bromomethylation with paraformaldehyde and HBr in acetic acid.[12] The product **2a** was produced in excellent yield and could be isolated as a crystalline, white solid in gram quantities from commercially available **DB24C8** (Scheme 1). Replacement of all four bromides by OR groups (R = $CH_2CH_2CH_3$, $CH_2(C_6H_5)$, C_6H_5 and C_6H_4(4-COOEt)) was accomplished using simple substitution chemistry involving exchange of bromide for alkoxide. The four new crown ethers were obtained as white crystalline solids in good yields (Scheme 1).

The new crown ethers **2b–2e** were characterized by ^{1}H NMR spectroscopy and ESI-MS. The major common characteristics of the ^{1}H NMR spectra were (1) the addition of a new resonance in the range 4.47–5.14 ppm due to the addition of a CH_2O methylene group, (2) simplification of the aromatic region in which only a single singlet resonance was now observed in the range of 6.95–7.10 ppm and (3) new resonances due to the appended R-groups.

X-ray quality crystals were obtained for **2d** and the structure is shown in Fig. 1. The structure has a crystallographically imposed centre of symmetry and the macrocycle adopts an open, S-shaped conformation which is similar to that found for **DB24C8**.[13] The pairs of $CH_2O(C_6H_5)$ groups on each aromatic ring are oriented on the same side of the catechol ring.

[2]Pseudorotaxane formation

Three representative 1,2-bis(pyridinium)ethane axles with phenyl, 4-pyridyl and 4-benzyl-pyridinum groups (**3a** X = C_6H_5, **3b** X = C_5H_4N, **3c**, X = $C_5H_4N^+Bn$) substituted at the 4-position of the pyridinium ring were used to determine the effect of crown ether substitutions on [2]pseudorotaxane formation (Scheme 2). Association constants (K_a) and binding energies ($\Delta G°$) for 12 new [2]pseudorotaxanes were measured in CD_3CN at 298 K by ^{1}H NMR spectroscopy using the single-point method appropriate for systems undergoing slow exchange on the NMR timescale. The results are summarized in Table 1 and compared to previously recorded values for **DB24C8**.[3g,n,14]

There are two basic trends observed for the association constants of these 12 interpenetrated molecules. Firstly, it is expected that the presence of four CH_2OR substituents would make the aromatic rings of the crown ether more electron rich

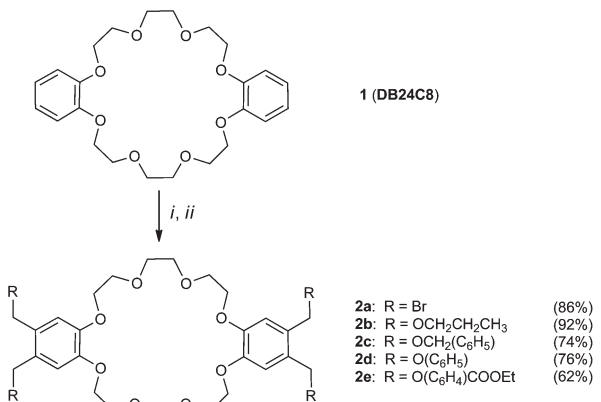

Scheme 1 Synthesis of tetra-substituted derivatives of **DB24C8**. (i) **2a**: $(CH_2O)_n$, 33% HBr/CH_3COOH, RT, 2 days, no stirring; (ii) **2b**, **2c**: ROH, **2a**, NaH, THF, reflux, 24 h; **2d**, **2e**: ROH, **2a**, K_2CO_3, CH_3CN, reflux, 5 days.

Fig. 1 Ball-and-stick representation of the single-crystal X-ray structure of crown ether macrocycle **2d**.

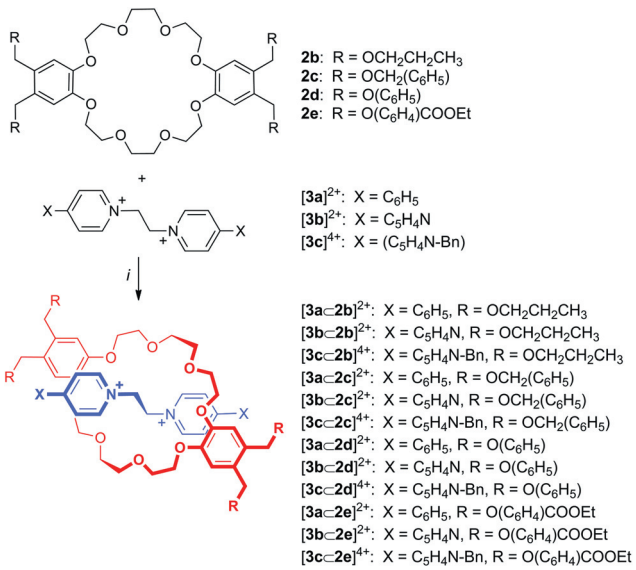

Scheme 2 Formation of [2]pseudorotaxanes. (i) CD_3CN, 2.0 × 10^{-3} M, 298 K. All counterions are triflate, ($OTf^- = CF_3SO_3^-$).

Table 1 Complete listing of K_a [a] and $\Delta G°$ values for [2]pseudorotaxanes in CD_3CN solution (2.0 × 10^{-3} M) at 298 K

[2]Pseudorotaxane	K_a [a] (×10^2 M^{-1})	$\Delta G°$ (kJ mol^{-1})
$[\mathbf{3a}\subset\mathbf{1}]^{2+}$	4.0	−14.8
$[\mathbf{3a}\subset\mathbf{2b}]^{2+}$	11.5	−17.5
$[\mathbf{3a}\subset\mathbf{2c}]^{2+}$	7.3	−17.1
$[\mathbf{3a}\subset\mathbf{2d}]^{2+}$	12.6	−17.7
$[\mathbf{3a}\subset\mathbf{2e}]^{2+}$	8.8	−16.8
$[\mathbf{3b}\subset\mathbf{1}]^{2+}$	9.3	−16.9
$[\mathbf{3b}\subset\mathbf{2b}]^{2+}$	18.0	−18.4
$[\mathbf{3b}\subset\mathbf{2c}]^{2+}$	6.6	−16.0
$[\mathbf{3b}\subset\mathbf{2d}]^{2+}$	16.2	−18.3
$[\mathbf{3b}\subset\mathbf{2e}]^{2+}$	11.9	−17.7
$[\mathbf{3c}\subset\mathbf{1}]^{4+}$	10.0	−10.0
$[\mathbf{3c}\subset\mathbf{2b}]^{4+}$	26.6	−19.6
$[\mathbf{3c}\subset\mathbf{2c}]^{4+}$	5.9	−16.7
$[\mathbf{3c}\subset\mathbf{2d}]^{4+}$	8.2	−16.6
$[\mathbf{3c}\subset\mathbf{2e}]^{4+}$	4.3	−15.1

[a] All values were recorded at 500 MHz and determined using the single point method applicable to slow exchange on the NMR timescale. Errors are estimated at <10%.

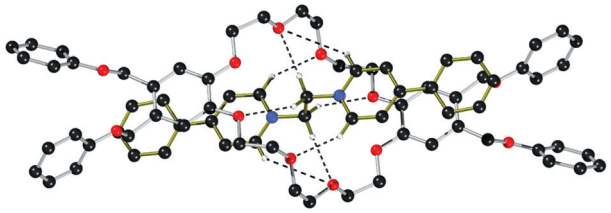

Fig. 2 Ball-and-stick representation of the single-crystal X-ray structure of [2]pseudorotaxane [**3a**⊂**2d**]$^{2+}$. Counterions and H-atoms not involved in hydrogen-bonding are omitted for clarity.

Downloaded by University of California - San Diego on 01 September 2012
Published on 14 May 2012 on http://pubs.rsc.org | doi:10.1039/C2OB25200G

resulting in an increase in the strength of the non-covalent interactions between these wheels and the three electron deficient axles. This is indeed the case for the smallest R-group, *n*-propyl, as an increase in association constant is observed with each axle relative to **DB24C8**.[3g] Secondly, [2]pseudorotaxane formation with the tetracationic axle [**3c**]$^{4+}$ would be predicted to be the most favourable due to increased ion–dipole interactions, but with crowns **2c**–**2e** the association constants are actually lower than were observed for **DB24C8**.[3g] It is thus likely that for larger and less flexible appendages, steric interactions between the axle and wheel are an overriding negative influence resulting in a reduced association constant. Although, this subtle interplay between electronic and steric effects makes it difficult to predict the degree of interaction between any single pair of axle and wheel, these observations are consistent with a straightforward thermodynamically driven molecular recognition event which results in [2]pseudorotaxane formation as described previously for simpler systems involving **DB24C8**.[3g,n,14]

The single-crystal X-ray structure of [2]pseudrotaxane [**3a**⊂**2d**][OTf]$_2$ was determined and the cationic portion is shown in Fig. 2. The dicationic axle [**3a**]$^{2+}$ is threaded through the central cavity of macrocycle **2d** and held in place *via* N$^+$···O ion–dipole interactions, a series of eight C–H···O hydrogen bonds and significant π-stacking interactions between the electron-poor pyridinium rings and electron-rich catechol rings. This is consistent with the interactions previously identified for [2]pseudorotaxanes containing **DB24C8**[3g] and observed in solution for this study with crown ethers **2b**–**2e**. The four substituents of crown ether **2d** are oriented to one side of the attached aromatic ring, similar to the structure of **2d**, with π-stacking of the axle pyridinium ring occurring on the opposite face; *i.e.* there are no significant intramolecular interactions between any of the six substituent phenyl groups on either the axle or the wheel.

[2]Rotaxane synthesis

[2]Pseudorotaxanes comprising pyridine terminated axle [**3b**]$^{2+}$ were alkylated with bulky *t*-butylbenzyl groups to yield permanently interlocked [2]rotaxanes [**4**⊂**2b**]$^{4+}$, [**4**⊂**2c**]$^{4+}$, [**4**⊂**2d**]$^{4+}$ and [**4**⊂**2e**]$^{4+}$ (Scheme 3).[15] The products could be isolated as orange-red solids in moderate yields after chromatography and counter-ion exchange to $CF_3SO_3^-$.

^{1}H NMR spectra for [2]rotaxanes [**4**⊂**2b**]$^{4+}$, [**4**⊂**2c**]$^{4+}$, [**4**⊂**2d**]$^{4+}$ and [**4**⊂**2e**]$^{4+}$ in CD_3CN show evidence of the original intramolecular interactions used to template the molecules which are now permanently a part of these interlocked species

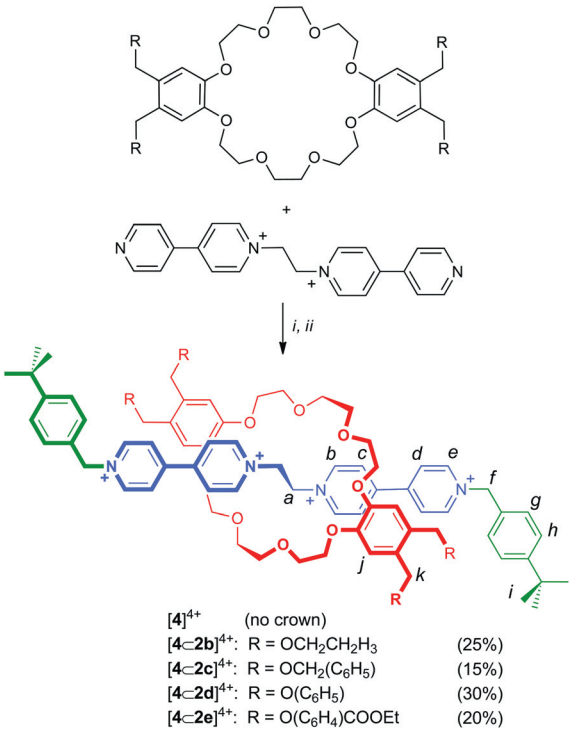

Scheme 3 Synthesis of [2]rotaxanes. (i) 5 : 1 eq. crown ether to eq. axle, 4 eq. of 4-*tert*-butylbenzyl bromide in CH_3CN, RT, 7 days. (ii) $MeNO_2$, sat'd [Na][CF_3SO_3](aq). Reported yields are after extensive work-up and chromatography. All counterions are triflate, (OTf$^-$ = $CF_3SO_3^-$).

(Table 2). In particular, resonances for ethylene protons *a* and α-pyridinium protons *b* are shifted to higher frequency (0.26–0.34 ppm) due to significant hydrogen-bonding, while shifts to lower frequencies (0.22–0.50 ppm) for pyridinium peaks *c* and *d* and catechol protons *j* can be attributed to π-stacking between the electron poor and electron rich aromatic rings. The chemical shift changes upon going from naked axle [**4**]$^{4+}$ to [2]rotaxane are identical to those observed upon formation of [**4**⊂**1**]$^{4+}$ which contains the parent crown ether **DB24C8**.[12] For the [2]rotaxanes with the most flexible R-groups on the wheel ([**4**⊂**2b**]$^{4+}$, [**4**⊂**2c**]$^{4+}$) there are no major differences in chemical shifts when incorporating a tetra-substituted crown ether in place of **DB24C8**. This infers that these groups, although presenting potential steric barriers to initial interpenetration, do not substantially impact the structure of the final interlocked molecule. There are, however, some differences observed for chemical shift data for the [2]rotaxanes with less flexible R-groups ([**4**⊂**2d**]$^{4+}$, [**4**⊂**2e**]$^{4+}$). It appears that the aromatic rings of the substituent R-groups interact with the benzylic *f* and aromatic *g* and *h* protons of the stopper shielding these groups resulting in shifts to lower frequency (0.17–0.41 ppm).

Single-crystal X-ray structures were determined for [2]rotaxanes [**4**⊂**2c**][OTf]$_4$ and [**4**⊂**2d**][OTf]$_4$ which contain four $CH_2OCH_2C_6H_5$ and $CH_2OC_6H_5$ groups respectively attached to the crown ether wheel. Figs. 3 and 4 show the cationic portions [**4**⊂**2c**]$^{4+}$ and [**4**⊂**2d**]$^{4+}$. In both structures, the terminal *tert*-butylbenzyl groups are bent away from and oriented on opposite sides of the central core of the [2]rotaxane. For [**4**⊂**2c**]$^{4+}$, the

 This journal is © The Royal Society of Chemistry 2012

View Online

Table 2 Selected ^{1}H NMR chemical shifts for crown ethers **2b–2e**, dumbbell $[\mathbf{4}]^{4+}$ and [2]rotaxanes $[\mathbf{4}\subset\mathbf{2b}]^{4+}$, $[\mathbf{4}\subset\mathbf{2c}]^{4+}$, $[\mathbf{4}\subset\mathbf{2d}]^{4+}$ and $[\mathbf{4}\subset\mathbf{2e}]^{4+}$ derived from pyridine terminated axle $[\mathbf{3b}]^{2+}$ [a]

	$\delta(\Delta\delta)$ Values (ppm)				
Proton	$[\mathbf{4}]^{4+}$	$[\mathbf{4}\subset\mathbf{2b}]^{4+}$	$[\mathbf{4}\subset\mathbf{2c}]^{4+}$	$[\mathbf{4}\subset\mathbf{2d}]^{4+}$	$[\mathbf{4}\subset\mathbf{2e}]^{4+}$
a	5.27	5.57 (+0.30)	5.57 (+0.30)	5.53 (+0.26)	5.61 (+0.34)
b	9.03	9.32 (+0.29)	9.32 (+0.29)	9.37 (+0.34)	9.36 (+0.33)
c	8.48	8.13 (−0.35)	8.14 (−0.34)	8.26 (−0.22)	8.23 (−0.25)
d	8.43	8.04 (−0.39)	7.93 (−0.50)	8.20 (−0.23)	8.17 (−0.26)
e	9.00	8.92 (−0.08)	8.53 (−0.47)	8.84 (−0.16)	8.86 (−0.14)
f	5.79	5.80 (+0.01)	5.81 (+0.02)	5.62 (−0.17)	5.62 (−0.17)
g	7.44	7.50 (+0.06)	7.39 (−0.05)	7.03 (−0.41)	7.25 (−0.19)
h	7.54	7.60 (+0.06)	7.53 (−0.01)	7.25 (−0.29)	7.35 (−0.19)
i	1.32	1.36 (+0.04)	1.30 (−0.02)	1.23 (−0.09)	1.22 (−0.10)
Proton	Crown	$[\mathbf{4}\subset\mathbf{2b}]^{4+}$	$[\mathbf{4}\subset\mathbf{2c}]^{4+}$	$[\mathbf{4}\subset\mathbf{2d}]^{4+}$	$[\mathbf{4}\subset\mathbf{2e}]^{4+}$
j (**2b**)	6.95	6.64 (−0.31)	—	—	—
j (**2c**)	6.95	—	6.69 (−0.26)	—	—
j (**2d**)	7.10	—	—	6.86 (-0.24)	—
j (**2e**)	7.10	—	—	—	6.86 (−0.24)
k (**2b**)	4.43	4.04 (−0.39)	—	—	—
k (**2c**)	4.47	—	4.11 (−0.36)	—	—
k (**2d**)	5.09	—	—	4.68 (−0.41)	—
k (**2e**)	5.14	—	—	—	4.76 (−0.38)

[a] All spectra were recorded at 500 MHz in MeCN-d_3 at 298 K. The labelling key can be found in Scheme 3.

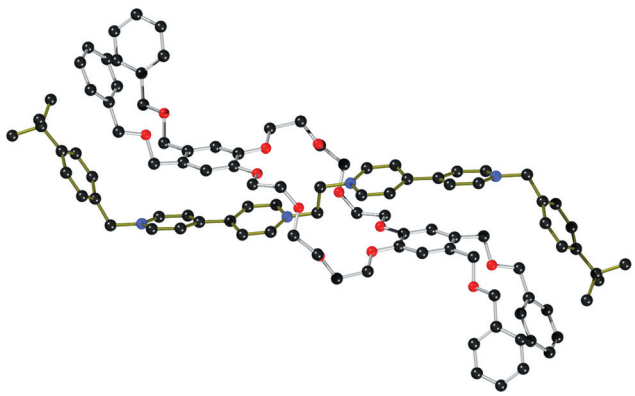

Fig. 3 Ball-and-stick representation of the single-crystal X-ray structure of [2]rotaxane $[\mathbf{4}\subset\mathbf{2c}]^{4+}$. Counterions and H-atoms are omitted for clarity.

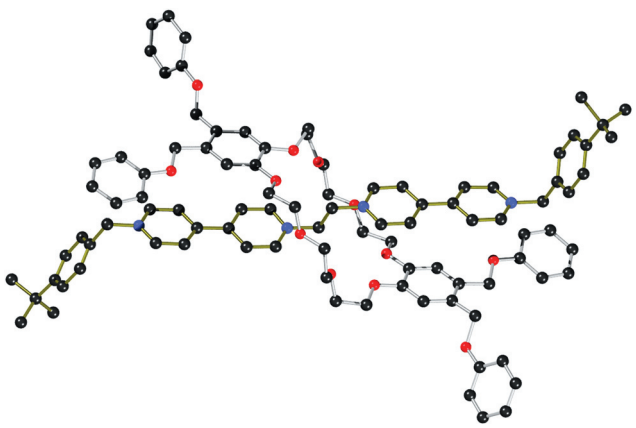

Fig. 4 Ball-and-stick representation of the single-crystal X-ray structure of [2]rotaxane $[\mathbf{4}\subset\mathbf{2d}]^{4+}$. Counterions and H-atoms are omitted for clarity.

$CH_2OCH_2C_6H_5$ groups are all positioned on the same side of the central core as the *tert*-butylbenzyl units. However, for $[\mathbf{4}\subset\mathbf{2d}]^{4+}$, one of the $CH_2OC_6H_5$ groups is oriented on the opposite side of the core, away from the *tert*-butylbenzyl stopper, while the other OC_6H_5 group is involved in C–H···π interactions between the benzylic CH_2 group of the stopper and the $CH_2OC_6H_5$ substituent aromatic ring. In order to be involved in this extra interaction between axle and wheel, the two components must be significantly misaligned – the angle between the vectors of the long axis of the axle and wheel is 23°, whereas this value is 6° for $[\mathbf{4}\subset\mathbf{1}]^{4+}$ and is only 7° in $[\mathbf{4}\subset\mathbf{2c}]^{4+}$ containing the more flexible $OCH_2C_6H_5$ groups.[15a] It is likely that orientation of the R-groups in the solid state is dictated to a large extent by optimizing crystal packing but the observed intramolecular interactions must contribute in some fashion to the co-conformational preference and overall stability of the [2]rotaxane.

Even though several large inflexible substituents might initially act as a steric barrier to the formation of a [2]pseudorotaxane, once the two components involved are permanently interlocked as a [2]rotaxane, optimization of non-covalent interactions will occur to stabilize the whole assembly. It was of interest then to examine the influence of these substituted crown ethers on the formation and structure of transition metal complexes[3l,h,5,16] and metal organic rotaxane framework materials[11,17] derived from these new [2]pseudorotaxane and [2]rotaxanes.

A [2]rotaxane terpyridine ligand and complexation with Ru^{2+}

It has been previously demonstrated that [2]pseudorotaxanes with terminal coordinating groups, such as $[\mathbf{3b}\subset\mathbf{DB24C8}]^{2+}$, are

Downloaded by University of California - San Diego on 01 September 2012
Published on 14 May 2012 on http://pubs.rsc.org | doi:10.1039/C2OB25200G

Published on 14 May 2012 on http://pubs.rsc.org | doi:10.1039/C2OB25200G
Downloaded by University of California - San Diego on 01 September 2012

capable of acting as ligands for transition metals, but care must be taken during synthesis to preserve the non-covalent interactions that stabilize the interpenetrated pair – by for example excluding heat or competitive solvents.[15a,17,18] Alternately, if the stopper of a [2]rotaxane contains a group for binding metals, the permanently interlocked [2]rotaxane can act directly as a ligand without the need for special precautions during synthesis.[16,19] This is especially relevant if complexation of an inert metal centre is targeted as these syntheses often require forcing conditions.[3c,h,19] We have previously prepared a [2]rotaxane ligand with a **DB24C8** wheel and stoppers that contains chelating terpyridine groups.[16c] Herein, we report an analogous [2]rotaxane ligand containing crown ether wheel **2e** and its subsequent coordination to two $[Ru(terpy)]^{2+}$ fragments.

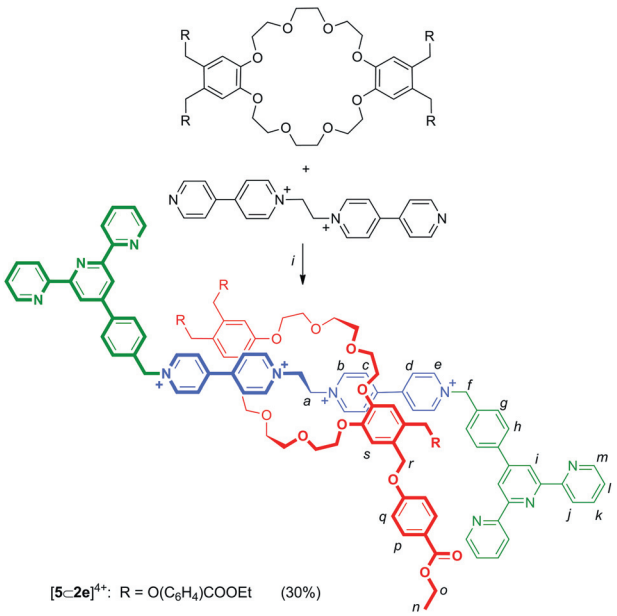

Scheme 4 Synthesis of [2]rotaxane ligand. (i) 2 equiv. of 4′-(4-bromobenzyl)-2,2′,6′,2″-terpyridine, $MeNO_2$, RT, 7 days followed by anion exchange by stirring the $MeNO_2$ layered with NaOTf(aq).

The [2]rotaxane ligand $[\mathbf{5}\subset\mathbf{2e}]^{4+}$, containing terpy chelating groups, was prepared in analogous fashion to the [2]rotaxanes $[\mathbf{4}\subset(\mathbf{2b–e})]^{4+}$ but using 4′-(4-bromobenzyl)-2,2′,6′,2″-terpyridine as the stoppering reagent in place of *tert*-butylbenzyl bromide (Scheme 4).[16c] The ^{1}H NMR spectrum of $[\mathbf{5}\subset\mathbf{2e}]^{4+}$ was similar to that observed for $[\mathbf{4}\subset\mathbf{2e}]^{4+}$ with addition peaks attributable to the two terpyridine groups (7.47–8.76 ppm).

As designed, $[\mathbf{5}\subset\mathbf{2e}]^{4+}$ is capable of acting as a binucleating ligand *via* two terminal terpyridine groups. Refluxing $[\mathbf{5}\subset\mathbf{2e}][OTf]_4$ with two equivalents of $[RuCl_3(terpy)]$ in an EtOH–H_2O solution produced, after anion exchange to triflate, the complex $[(Ru(terpy))_2(\mathbf{5}\subset\mathbf{2e})][OTf]_8$. The ^{1}H NMR data for dumbbell $[\mathbf{5}]^{4+}$, [2]rotaxane ligand $[\mathbf{5}\subset\mathbf{2e}]^{4+}$ and the Ru(II) complexes $[(Ru(terpy))_2(\mathbf{5})]^{8+}$ and $[(Ru(terpy))_2(\mathbf{5}\subset\mathbf{2e})]^{8+}$ are summarized in Table 3. The chemical shift differences between the dumbbell $[\mathbf{5}]^{4+}$ and the [2]rotaxane $[\mathbf{5}\subset\mathbf{2e}]^{4+}$ are similar to those observed for the [2]rotaxanes $[\mathbf{4}\subset(\mathbf{2b–e})]^{4+}$; protons *a* and *b* are shifted to higher frequency (0.32–0.35 ppm) due to hydrogen-bonding, while pyridinium peaks *c* and *d* and catechol protons *s* shift to lower frequencies (0.19–0.22 ppm) due to π-stacking. Coordination to Ru(II) yielding $[(Ru(terpy))_2(\mathbf{5})]^{8+}$, causes significant coordination shifts to lower frequencies for terpyridine protons *j* – *m* (0.06–1.29 ppm) with the largest shift for proton *m* being attributed to the change in ligand conformation from transoid to cisoid. For $[(Ru(terpy))_2(\mathbf{5}\subset\mathbf{2e})]^{8+}$, similar chemical shift changes are observed due to a combination of both rotaxane formation and coordination to Ru(II).[16c]

The single-crystal X-ray structures of both $[\mathbf{5}\subset\mathbf{2e}][OTf]_4$ and $[(Ru(terpy))_2(\mathbf{5}\subset\mathbf{2e})][OTf]_8$ were determined and the cationic portions of these molecules are shown in Fig. 5. In both structures, pairs of $CH_2OC_6H_4$(4-COOEt) groups on the ends of each

Table 3 Selected ^{1}H NMR chemical shifts for dumbbell $[\mathbf{5}]^{4+}$, [2]rotaxane $[\mathbf{5}\subset\mathbf{2e}]^{4+}$ and complexes $[(Ru(terpy))_2(\mathbf{5})]^{8+}$ and $[(Ru(terpy))_2(\mathbf{5}\subset\mathbf{2e})]^{8+}$ [a]

	$\delta(\Delta\delta)$ Values (ppm)			
Proton	$[\mathbf{5}]^{4+}$	$[\mathbf{5}\subset\mathbf{2e}]^{4+}$	$[(Ru(terpy))_2(\mathbf{5})]^{8+}$	$[(Ru(terpy))_2(\mathbf{5}\subset\mathbf{2e})]^{8+}$
a	5.27	5.62 (+0.35)	5.34 (+0.07)	5.67 (+0.40)
b	9.04	9.36 (+0.32)	9.19 (+0.15)	9.43 (+0.39)
c	8.49	8.27 (−0.22)	8.58 (+0.09)	8.42 (−0.07)
d	8.46	8.27 (−0.19)	8.58 (+0.12)	8.42 (−0.04)
e	9.04	8.98 (−0.06)	9.14 (+0.10)	9.11 (+0.07)
f	5.94	5.77 (−0.17)	6.04 (+0.10)	5.87 (−0.07)
g	7.71	7.71 (0.00)	7.88 (+0.17)	8.09 (+0.38)
h	8.04	7.52 (−0.52)	8.34 (+0.30)	7.69 (−0.35)
i	8.76	8.57 (−0.19)	9.03 (+0.27)	8.83 (−0.07)
j	8.70	8.73 (+0.03)	8.50 (−0.20)	8.51 (−0.19)
k	7.98	7.99 (+0.01)	7.92 (−0.06)	7.92 (−0.06)
l	7.46	7.47 (+0.01)	7.16 (−0.30)	7.19 (−0.25)
m	8.70	8.70 (0.00)	7.41 (−1.29)	7.45 (−1.25)
Proton	**2e**[b]	$[\mathbf{5}\subset\mathbf{2e}]^{4+}$	$[(Ru(terpy))_2(\mathbf{5})]^{8+}$	$[(Ru(terpy))_2(\mathbf{5}\subset\mathbf{2e})]^{8+}$
p	7.90	7.88 (−0.02)	—	7.92 (+0.02)
q	7.03	6.94 (−0.09)	—	7.03 (0.00)
r	5.14	4.64 (−0.50)	—	4.81 (−0.33)
s	7.10	6.84 (−0.16)	—	6.92 (−0.18)

[a] All spectra were recorded at 500 MHz in MeCN-d_3 at 298 K. The labelling key can be found in Scheme 4. [b] Shifts are from **2e**.

 This journal is © The Royal Society of Chemistry 2012

Downloaded by University of California - San Diego on 01 September 2012
Published on 14 May 2012 on http://pubs.rsc.org | doi:10.1039/C2OB25200G

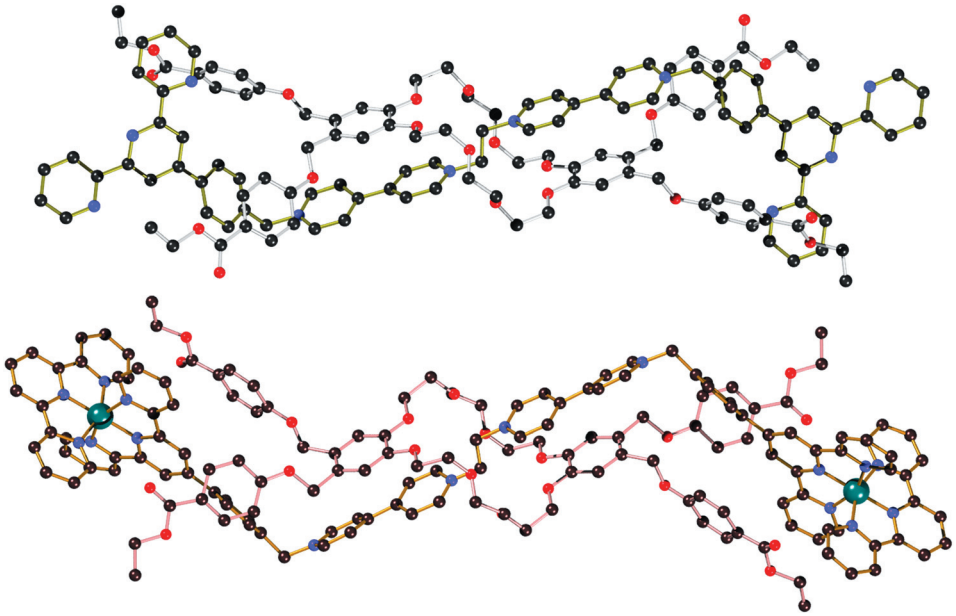

Fig. 5 Top: A ball-and-stick representation of the single-crystal X-ray structure of [2]rotaxane ligand [**5⊂2e**]$^{4+}$. Bottom: A ball-and-stick representation of the single-crystal X-ray structure of binuclear complex [(Ru(terpy))$_2$(**5⊂2e**)]$^{8+}$. Counterions and H-atoms are omitted for clarity.

crown ether bracket the stoppering group with one $CH_2OC_6H_4$(4-COOEt) substituent involved in π-stacking with a pyridine group of the terpy stopper and the other interacting with the linking phenyl unit (protons *g* and *h*) *via* an edge-on C–H···π interaction. Thus, the longer, functionalized stoppers on the axle are capable of interacting directly with the extended substituents of the wheel in an intramolecular fashion. This concept could potentially be used to link axle and wheel *via* coordination chemistry or perhaps use a wheel donor as a hemi-labile ligand.

A metal–organic rotaxane framework

[2]Pseudorotaxanes and [2]rotaxanes have also been used as ligand/linkers in the creation of metal–organic framework (MOF) materials.[11,17] However, to date, there have been no reports of a metal–organic *rotaxane* framework (MORF) in which the skeletal framework could be kept constant and the nature of the interlocked wheel component varied in order to observe the effect on structure and/or materials properties. This is undoubtedly because very few MORFs are known as their synthesis/crystallization is often difficult. We previously reported a MORF which is a 2D network comprised of [**3b⊂DB24C8**]$^{2+}$ linkers and $[Cd(H_2O)_2]^{2+}$ nodes.[17a] In an attempt to prepare an analogous MORF with a tetra-substituted crown ether, 2 equivalents of [**3b⊂2d**][BF_4]$_2$ were combined with 1 equivalent of $[Cd(H_2O)_6][BF_4]_2$ in $MeNO_2$ solution which after partial evaporation produced a yellow crystalline material in ~40% yield.

Single-crystal X-ray crystallography showed this material to have formula {[$Cd(H_2O)_2$(**3b⊂2d**)(**3b**)][BF_4]$_6$·($MeNO_2$)$_{23}$}. The structure is a 2D network, as designed, with [**3b**]$^{2+}$ linkers joining $[Cd(H_2O)_2]^{2+}$ metal centres (Fig. 6). This is exactly the same square grid arrangement previously observed for {[Cd(H_2O)(BF_4)(**3b⊂DB24C8**)$_2$]}$_n$ when [**3b⊂DB24C8**]$^{2+}$ was used as the linker allowing for direct comparison of two MORFs that differ only by the nature of their crown ether wheel.[17a]

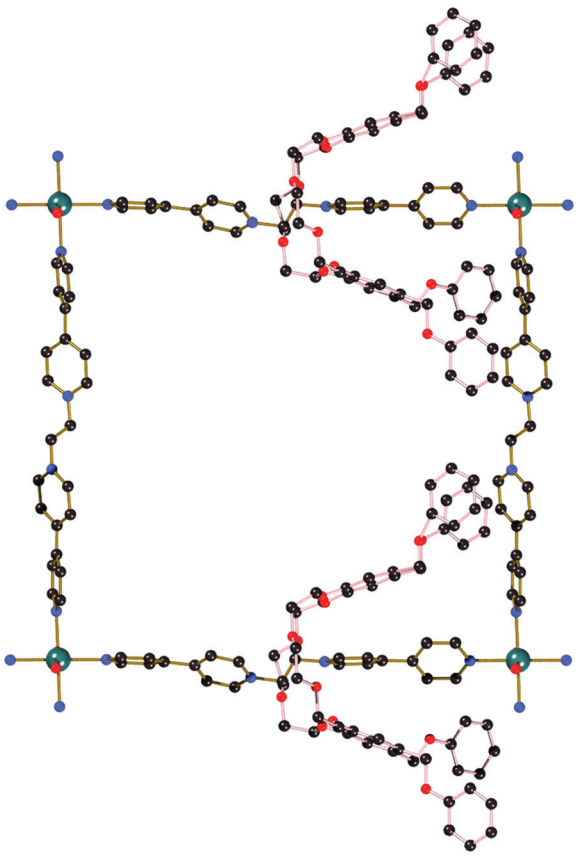

Fig. 6 Ball-and-stick representation of the single-crystal X-ray structure of metal–organic rotaxane framework [$Cd(H_2O)_2$(**3b⊂2d**)(**3b**)]$_n$ showing one square grid. Counterions and H-atoms are omitted for clarity.

The major difference between the two square grid structures is that the new version containing crown ether **2d** with four

Published on 14 May 2012 on http://pubs.rsc.org | doi:10.1039/C2OB25200G
Downloaded by University of California - San Diego on 01 September 2012

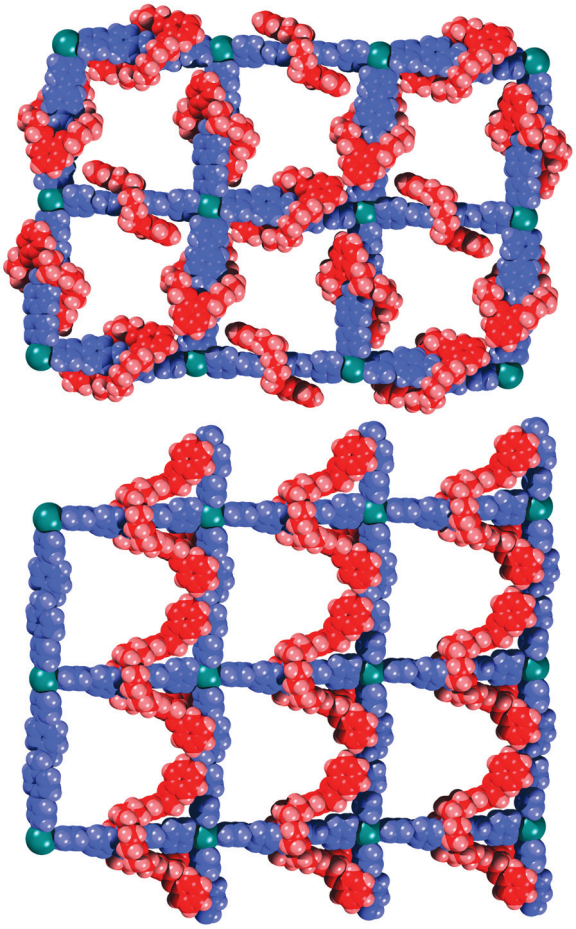

Fig. 7 Space-filling representation of a 2 × 3 section of the 2D square network of: top, previously reported $[Cd(H_2O)(BF_4)(\mathbf{3b}\subset\mathbf{DB24C8})_2]_n$ and bottom, $[Cd(H_2O)_2(\mathbf{3b}\subset\mathbf{2d})(\mathbf{3b})]_n$ (this work).

$CH_2OC_6H_5$ groups has one of the axle linkers missing the crown ether; *i.e.* one of the linkers is not a rotaxane but a naked axle.[17b] It appears as that the four $CH_2OC_6H_5$ appendages on an adjacent rotaxane take on the role of sheltering the axle normally accomplished by threading on a wheel and rotaxane formation. Fig. 7 shows space-filling views of the two 2D MORFs. The axle and the metal components yield two MORFs with identical metal–organic frameworks while the interlocked wheel component can be thought of as a supramolecular additive which does not perturb the structure of the coordination polymer. It may be possible to use this as method to tune the internal properties and/or structure of the cavities in porous MORFs – for example making them hydrophobic or hydrophilic depending on the crown ether substituents. Preliminary results from a poorly resolved X-ray structure involving the same metal and axles with crown ether **2b**, containing smaller *n*-propyl groups, appears to show that all linkers are rotaxanes analogous to the previously reported MORF $[Cd(H_2O)(BF_4)(\mathbf{3b}\subset\mathbf{DB24C8})_2]_n$ (top, Fig. 7). If so, this would infer that large groups such as those in $[Cd(H_2O)_2(\mathbf{3b}\subset\mathbf{2d})(\mathbf{3b})]_n$ (top, Fig. 7) are required to compensate for rotaxane formation and that smaller more flexible groups might perhaps be better for full saturation and filling the internal pores usually occupied by solvent. Work in this concept is ongoing.

Conclusions

Derivatives of the ubiquitous macrocycle **DB2C8** containing four CH_2OR groups appended to the two aromatic rings are readily available in good yield following two simple steps from commercially available starting materials. The formation of [2]pseudorotaxanes with 1,2-bis(pyridinium)ethane axles is favourable in acetonitrile solvent and association constants are comparable to those for the same axles with **DB24C8**. Simple [2]rotaxanes and [2]rotaxane ligands with terpyridine groups can be prepared *via* the threading-followed-by-stoppering methodology. Coordination to an inert Ru(II) metal centre was shown to be straightforward and it was established that the appendages from a substituted crown ether wheel are capable of interacting with these coordination sites. Most significantly it was demonstrated that a series of structurally related metal–organic rotaxane frameworks (MORFs) is possible in which the crown ether component can be thought of as a supramolecular additive for potentially tuning the internal properties of these porous materials.

Experimental

General

Phenol, benzyl alcohol, ethyl(4-hydroxy)benzoate, 4-*tert*-butylbenzyl bromide, sodium triflate, sodium borohydride, **DB24C8**, 2,2′ : 6′,2″-terpyridine, $RuCl_3{\cdot}xH_2O$, and cadmium(II) tetrafluoroborate were obtained from Sigma-Aldrich and used as received. Axles[3g] $[\mathbf{3a}][OTf]_2$, $[\mathbf{3b}][OTf]_2$ and $[\mathbf{3c}][OTf]_2$, $[RuCl_3(terpy)]$[20] and 4′-(4-bromobenzyl)-2,2′,6′,2″-terpyridine[21] were synthesized according to literature procedures. Deuterated solvents were obtained from Cambridge Isotope Laboratories and used as received. Solvents were dried using an Innovative Technologies Solvent Purification System. Thin layer chromatography (TLC) was performed using Merck Silica gel 60 F_{254} plates and viewed under UV light. Column chromatography was performed using Silicycle Ultra Pure Silica Gel (230–400 mesh). ^{1}H NMR experiments were performed on a Bruker Avance 500 instrument using the deuterated solvent as lock and the residual solvent or TMS as the internal reference. High-resolution mass spectrometry experiments were performed on a Micromass LCT electro-spray-ionization time-of-flight mass spectrometer in lock-mass mode. Solutions of 50–100 ng μL^{-1} were prepared in MeCN–H_2O (1 : 1) (unless otherwise indicated) and injected for analysis at a rate of 5 $\mu L\ min^{-1}$ using a syringe pump.

Preparation of crown ether 2a. DB24C8 (0.200 g, 0.446 mmol), paraformaldehyde (0.121 g, 4.01 mmol) and 33% hydrobromic acid in acetic acid (1.3 mL) were stirred until all the solids had dissolved. The mixture was then left to stand without stirring for 3 days while a white precipitate formed. The solid was collected by filtration, washed consecutively with water, ethanol, and diethyl ether and then air dried. The solid was recrystallized from MeCN. Yield: 0.316 g, 86%. MP: 201–205 °C. ^{1}H NMR (500 MHz, $CDCl_3$): δ 6.83 (4H, s), 4.59 (8H, s), 4.15 (8H, m), 3.90 (8H, m), 3.79 (8H, m).

Preparation of crown ether 2b. Sodium metal was dissolved in dry *n*-propanol (30 mL) and **2a** (1.00 g, 1.21 mmol) added with stirring under N_2. The mixture was refluxed for 12 h. After

 This journal is © The Royal Society of Chemistry 2012

Downloaded by University of California - San Diego on 01 September 2012
Published on 14 May 2012 on http://pubs.rsc.org | doi:10.1039/C2OB25200G

cooling, H_2O was added drop-wise with great care to destroy any excess Na(s). The solvent was evaporated and the residue partitioned between CH_2Cl_2 and H_2O. The organic layer was washed with H_2O (2 × 50 mL) and then dried with anhydrous $MgSO_4$. Yield: 0.828 g, 92%. MP: 72–75 °C. ^{1}H NMR (500 MHz, CD_3CN): δ 6.95 (4H, s), 4.43 (8H, s), 4.10 (8H, m), 3.78 (8H, m), 3.67 (8H, s), 3.39 (8H, t, J = 6.6 Hz), 1.57 (8H, m, J = 6.6, 7.3 Hz), 0.91 (12H, q, J = 7.3 Hz). ^{13}C NMR (125 MHz, CD_3CN): δ 148.5, 130.8, 115.3, 72.4, 71.4, 70.3, 70.2, 69.6, 23.5, 10.8. ESI-MS: m/z [**2b** + K]$^+$ calcd 775.4035, found 775.4007.

Preparation of crown ether 2c. NaH (118 mg, 4.88 mmol) and benzyl alcohol (527 mg, 4.88 mmol) in dry THF (30 mL) were stirred for 2 h at room temperature followed by the addition of **2a** (1.00 g, 1.21 mmol). The mixture was refluxed for 1.5 days, cooled to room temperature and H_2O (4 mL) added with care. THF was removed under vacuum and the residual oil dissolved in CH_2Cl_2 (50 mL) and washed with 1 M $NaHCO_3$ (3 × 50 mL) and H_2O (50 mL) and then dried with anhydrous $MgSO_4$. The CH_2Cl_2 was removed and the residue stirred in diethyl ether. Yield: 0.836 g, 74%. MP: 60–63 °C. ^{1}H NMR (500 MHz, CD_3CN): δ 7.31 (20H, m), 6.95 (4H, s), 4.47 (8H, s), 4.45 (8H, s), 4.09 (8H, m), 3.76 (8H, m), 3.65 (8H, s). ^{13}C NMR (125 MHz, CD_3CN): δ 148.6, 144.4, 130.4, 129.1, 128.5, 128.2, 115.6, 72.6, 71.4, 70.2, 69.9, 69.6. ESI-MS: m/z [**2c** + K]$^+$ calcd 967.4035, found 967.4070.

Preparation of crown ether 2d. To a solution of **2a** (1.00 g, 1.22 mmol) and phenol (0.459 g, 4.88 mmol) in CH_3CN (30 mL) was added K_2CO_3 and the mixture stirred under N_2 at reflux for 5 days. The solvent was evaporated and the residue partitioned between CH_2Cl_2 and H_2O. The organic layer was washed with H_2O (2 × 50 mL), dried with anhydrous $MgSO_4$ and recrystallized from CH_3CN. X-Ray quality crystals were grown by the slow diffusion of hexanes into a saturated $CHCl_3$ solution. Yield: 0.806 g, 76%. MP: 135–136 °C. ^{1}H NMR (500 MHz, CD_3CN): δ 7.27 (8H, t, J = 8.0 Hz), 7.03 (4H, s), 6.92 (12H, m), 5.05 (8H, s), 4.14 (8H, m), 3.85 (8H, m), 3.78 (8H, m). ^{13}C NMR (125 MHz, CD_2Cl_2): δ 159.0, 148.9, 129.7, 128.6, 121.2, 115.6, 71.4, 70.0, 69.7, 67.8. ESI-MS: m/z [**2d** + Na]$^+$ calcd 895.3669, found 895.3658.

Preparation of crown ether 2e. To a solution of **2a** (1.00 g, 1.22 mmol) and ethyl(4-hydroxy)benzoate (0.810 g, 4.88 mmol) in degassed MeCN (30 mL) was added K_2CO_3 and the mixture stirred under N_2 at reflux for 5 days. The solvent was then evaporated and the residue partitioned between CH_2Cl_2 and H_2O. The organic layer was washed with H_2O (2 × 50 mL) and then dried with anhydrous $MgSO_4$ and recrystallized from CH_3CN. Yield: 0.877 g, 62%. MP: 120–123 °C. ^{1}H NMR (500 MHz, CD_3CN): δ 7.95 (8H, d, J = 8.4 Hz), 7.03 (4H, s), 6.97 (8H, d, J = 8.4 Hz), 5.11 (8H, s), 4.30 (8H, q, J = 7.0 Hz), 4.15 (8H, m), 3.85 (8H, m), 3.75 (8H, m), 1.35 (12H, t, J = 7.0 Hz). ^{13}C NMR (125 MHz, CD_2Cl_2): δ 166.5, 162.7, 149.4, 131.9, 128.3, 124.0, 116.0, 114.9, 71.6, 70.3, 70.0, 68.3, 61.1, 14.7. ESI-MS: m/z [**2e** + Na]$^+$ calcd 1183.4515, found 1183.4524.

Preparation of [2]rotaxane [4⊂2b][OTf]$_4$. **3b**[OTf]$_2$ (0.050 g, 0.078 mmol), **2b** (0.115 g, 0.157 mmol) were dissolved in CH_3CN (10 mL) and stirred overnight. 4-*t*-Butylbenzyl bromide (0.150 g, 0.660 mmol) was added and the mixture stirred for 4 days. The solvent was removed and the residue stirred in CH_2Cl_2 (25 mL) for 30 min. The solid that remained was filtered and the filtrate was evaporated. The orange solid was dissolved in a two layer solution of $MeNO_2$/NaOTf(aq) and stirred overnight. The organic layer was separated and dried with anhydrous $MgSO_4$. The CH_3NO_2 solution was filtered and the solvent evaporated. The residue was stirred in toluene. Yield 0.038 g, 25%. MP: 183–190 °C (dec). NMR (500 MHz, CD_3CN): δ 9.32 (4H, d, J = 5.9 Hz), 8.92 (4H, d, J = 6.9 Hz), 8.13 (4H, d, J = 6.9 Hz), 8.04 (4H, d, J = 6.8 Hz), 7.60 (4H, d, J = 8.4 Hz), 7.50 (4H, d, J = 8.4 Hz), 6.64 (4H, s), 5.80 (4H, s), 5.57 (4H, s), 4.04–3.94 (32H, m), 3.23 (4H, t, J = 6.7 Hz), 1.54 (8H, dd, J = 6.7, 7.4 Hz), 1.36 (12H, s), 0.90 (12H, t, J = 7.4 Hz). ESI-MS: m/z [**4⊂2b** + 2OTf]$^{2+}$ calcd 834.3731, found 834.3736.

Preparation of [2]rotaxane [4⊂2c][OTf]$_4$. **3b**[OTf]$_2$ (0.050 g, 0.078 mmol), **2c** (0.145 g, 0.157 mmol) was dissolved in CH_3CN (10 mL) and stirred overnight. 4-*t*-Butylbenzylbromide (0.150 g, 0.660 mmol) was added, and stirred for 4 days. The solvent was removed, and was stirred in CH_2Cl_2 (25 mL) for 30 minutes. The solid that remained was filtered, and the filtrate was evaporated. The orange solid was dissolved in a two layer solution of $MeNO_2$/NaOTf(aq) stirred overnight. The organic layer was separated, dried with $MgSO_4$. The CH_3NO_2 solution was filtered and solvent evaporated. The residue was stirred in toluene. X-ray quality crystals were grown by the slow diffusion of isopropyl ether into a saturated CH_3CN solution. Yield 0.025g, 15%. MP: 177–185 °C (dec). ^{1}H NMR (500 MHz, CD_3CN): δ 9.32 (4H, d, J = 6.8), 8.53 (4H, d, J = 6.8), 8.14 (4H, d, J = 6.8), 7.93 (4H, d, J = 6.8), 7.53 (4H, d, J = 8.4), 7.38–7.35 (12H, m), 7.31–7.28 (8H, m), 6.67 (4H, s), 5.55 (4H, s), 5.47 (4H, s), 4.35 (8H, s), 4.11 (8H, s), 4.04–3.99 (24H, m), 1.28 (18H, s). ESI-MS: m/z [**4⊂2c** + 2OTf]$^{2+}$ calcd 930.3731, found 930.3765.

Preparation of [2]rotaxane [4⊂2d][OTf]$_4$. **3b**[OTf]$_2$ (0.050 g, 0.078 mmol) and **2d** (0.140 g, 0.160 mmol) were dissolved in CH_3CN (10 mL) and stirred overnight. 4-*tert*-Butylbenzyl bromide (0.150 g, 0.660 mmol) was added and the mixture stirred for 4 days. The solvent was removed and the residue was stirred with CH_2Cl_2 (25 mL) for 30 minutes. The solid that remained was removed and the filtrate evaporated. The resulting orange solid was dissolved in a two layer solution of $MeNO_2$/NaOTf(aq) and stirred overnight. The organic layer was separated and dried with anhydrous $MgSO_4$. The CH_3NO_2 solution was filtered and solvent evaporated. The residue was stirred in toluene. X-ray quality crystals were grown by the slow diffusion of iso-propyl ether into a saturated CH_3CN solution. Yield 0.030 g, 30%. MP: 181–185 °C (dec). ^{1}H NMR (500 MHz, CD_3CN): δ 9.37 (4H, d, J = 6.6 Hz), 8.84 (4H, d, J = 6.6 Hz), 8.26 (4H, d, J = 6.6 Hz), 8.20 (4H, d, J = 6.6 Hz), 7.35 (8H, dd, J = 8.0 Hz), 7.25 (4H, d, J = 7.7 Hz), 7.03 (4H, d, J = 7.7 Hz), 6.92 (8H, d, J = 8.0 Hz), 6.86 (8H, s), 5.62 (8H, s), 5.53 (8H, s), 4.68 (8H, s), 4.08–4.02 (24H, m), 1.23 (18H, s). ESI-MS: m/z [**4⊂2d** + OTf]$^{3+}$ calcd 551.9104, found 551.9100.

Preparation of [2]rotaxane [4⊂2e][OTf]$_4$. **3b**[OTf]$_2$ (0.050 g, 0.078 mmol) and **2e** (0.185 g, 0.159 mmol) were dissolved in

CH_3CN (10 mL) and 4-*t*-butylbenzyl bromide (0.150 g, 0.660 mmol) added. The mixture was stirred for 4 days. The solvent was removed and the residue was stirred in CH_2Cl_2 (25 mL) for 30 min. The solid that remained was filtered and the filtrate was evaporated. The remaining orange solid was dissolved in a two layer solution of $MeNO_2$/NaOTf(aq) and stirred overnight. The organic layer was separated and dried with anhydrous $MgSO_4$. The CH_3NO_2 was removed by evaporation and the residue stirred in toluene. X-ray quality crystals were grown by the slow diffusion of iso-propyl ether into a saturated CH_3CN solution. Yield 0.037 g, 20%. MP: 188–193 °C (dec). ^{1}H NMR (500 MHz, CD_3CN): δ 9.36 (4H, d, J = 6.8 Hz), 8.86 (4H, d, J = 6.9 Hz), 8.23 (4H, d, J = 6.8 Hz), 8.17 (4H, d, J = 6.6 Hz), 7.99 (8H, d, J = 8.8 Hz), 7.35 (8H, d, J = 8.3 Hz), 7.25 (8H, d, J = 8.3 Hz), 6.97 (8H, d, J = 8.8 Hz), 6.86 (4H, s), 5.62 (4H, s), 5.61 (4H, s), 4.76 (8H, s), 4.33 (8H, q, J = 7.1 Hz), 4.02–4.08 (24H, m), 1.36 (8H, t, J = 7.1 Hz), 1.22 (18H, s). ESI-MS: m/z [**4⊂2e** + OTf]$^{3+}$ calcd 647.9385, found 647.9409.

Preparation of [2]rotaxane, [5⊂2e][OTf]$_4$. **3b**$[OTf]_2$ (0.050 g, 0.078 mmol) and **2e** (0.185 g, 0.159 mmol) were dissolved in $MeNO_2$ (10 mL) and stirred overnight. 4′-(4-Bromobenzyl)-2,2′,6′,2″-terpyridine (0.189 g, 0.147 mmol) was dissolved in CH_2Cl_2, and the mixture was stirred for 7 days. The organic layer was removed, and the orange solid stirred between $MeNO_2$ and NaOTf(aq) stirred overnight. The organic layer was separated, dried with anhydrous $MgSO_4$ and evaporated. The residue was stirred in toluene. The orange solid was dissolved in

Table 4 A summary of crystal data collection, solution and structure refinement parameters for single-crystal structure determinations

Compound	**2d**·($CHCl_3$)	[**3a⊂2d**][BF_4]$_2$·(CH_3NO_2)$_6$	[**4⊂2c**][OTf]$_4$·(H_2O)$_2$	[**4⊂2d**][OTf]$_4$·(CH_3CN)$_{3.5}$(H_2O)$_{1.5}$
CCDC number	864512	864511	864513	864507
Formula	$C_{53}H_{57}Cl_3O_{12}$	$C_{82}H_{94}B_2F_8N_8O_{24}$	$C_{104}H_{116}F_{12}N_4O_{26}S_4$	$C_{107}H_{119.5}F_{12}N_{7.5}O_{25.5}S_4$
Formula weight	992.34	1749.27	2194.25	2274.84
Crystal system	Triclinic	Monoclinic	Monoclinic	Triclinic
Space group	$P\bar{1}$ (2)	$C2/c$ (15)	$C2/c$ (15)	$P\bar{1}$ (2)
T (K)	173(2)	173(2)	173(2)	173(2)
a (Å)	12.554(4)	37.627(6)	27.729(3)	16.478(4)
b (Å)	13.774(5)	12.680(2)	16.863(2)	17.317(4)
c (Å)	15.329(5)	20.775(3)	23.505(3)	22.065(5)
α (°)	80.404(5)	—	—	78.7863)
β (°)	68.495(4)	123.038(2)	106.757(1)	78.864(3)
γ (°)	89.969(5)	—	—	65.622(3)
V (Å^3)	2426.4(15)	8309(2)	10 524(2)	5580(2)
Z	2	4	4	2
ρ, g cm^{-3}	1.358	1.398	1.385	1.354
μ, mm^{-1}	0.253	0.114	0.188	0.180
Reflections	8433	8470	8956	19 587
Variables/restraints	565/0	451/55	757/275	1462/537
R_1 [$I > 2\sigma(I)$][a]	0.1434	0.1216	0.1090	0.1114
R_1 (all data)	0.2106	0.1669	0.1499	0.1636
R_2w [$I > 2\sigma(I)$][b]	0.3560	0.3558	0.2910	0.3178
R_2w (all data)	0.3936	0.3818	0.3206	0.3647
GoF on F^2	1.165	1.296	1.097	1.291

Compound	[**5⊂2e**][OTf]$_4$·(CH_3CN)$_2$(H_2O)$_7$	[(Ru(terpy))$_2$(**5⊂2e**)][OTf]$_8$·(CH_3CN)$_2$(H_2O)$_3$	[Cd(H_2O)$_2$(**3b⊂2d**)(**3b**)][BF_4]$_6$·(CH_3NO_2)$_{23}$
CCDC number	864510	864509	864508
Formula	$C_{138}H_{144}F_{12}N_{12}O_{39}S_4$	$C_{172}H_{158}F_{24}N_{18}O_{47}Ru_2S_8$	$C_{119}H_{169}B_6CdF_{24}N_{31}O_{60}$
Formula weight	2950.90	4143.78	3627.11
Crystal system	Monoclinic	Monoclinic	Monoclinic
Space group	$P2_1/c$ (14)	$P2_1/n$ (14)	Pc (7)
T (K)	173(2)	173(2)	173(2)
a (Å)	21.417(3)	18.248(9)	20.057(3)
b (Å)	25.553(3)	20.018(10)	22.223(3)
c (Å)	13.838(2)	28.528(14)	18.474(3)
α (°)	—	—	—
β (°)	103.228(2)	92.355(8)	109.497(2)
γ (°)	—	—	—
V (Å^3)	7372(2)	10 412(9)	7763(2)
Z	2	2	2
ρ, g cm^{-3}	1.329	1.322	1.552
μ, mm^{-1}	0.161	0.321	0.270
Reflections	12 927	10 811	27 335
Variables/restraints	920/0	709/596	1174/534
R_1 [$I > 2\sigma(I)$][a]	0.1361	0.226	0.0855
R_1 (all data)	0.2414	0.4242	0.1188
R_2w [$I > 2\sigma(I)$][b]	0.2818	0.4545	0.2214
R_2w (all data)	0.3449	0.5573	0.2405
GoF on F^2	1.104	1.292	0.929

[a] $R_1 = \Sigma\,||F_o| - |F_c||/\,\Sigma\,|F_o|$. [b] $R_2w = [\Sigma[w(F_o^2 - F_c^2)^2]/\Sigma[w(F_o^2)^2]]^{1/2}$, where $w = q[\sigma^2(F_o^2) + (aP)^2 + bP]^{-1}$.

Downloaded by University of California - San Diego on 01 September 2012
Published on 14 May 2012 on http://pubs.rsc.org | doi:10.1039/C2OB25200G

 This journal is © The Royal Society of Chemistry 2012

Downloaded by University of California - San Diego on 01 September 2012
Published on 14 May 2012 on http://pubs.rsc.org | doi:10.1039/C2OB25200G

CH_3CN and *iso*-propyl ether was slowly diffused into the solution to give an orange solid. Yield: 0.065 g, 30%. MP: 166–172 °C (dec). ^{1}H NMR (500 MHz, CD_3CN): δ 9.36 (4H, d, J = 6.7 Hz), 8.98 (4H, d, J = 6.7 Hz), 8.73 (4H, d, J = 4.5 Hz), 8.70 (4H, d, J = 7.8 Hz), 8.57 (4H, s), 8.27 (4H, m), 8.00 (4H, d, J = 8.1, 1.7 Hz), 7.87 (8H, d, J = 8.8 Hz), 7.71 (4H, d, J = 8.0 Hz), 7.52 (4H, d, J = 8.0 Hz), 7.46 (4H, dd, J = 7.8, 1.7 Hz), 6.93 (4H, d, J = 8.8 Hz), 6.84 (4H, s), 5.77 (4H, s), 5.62 (4H, s), 4.64 (8H,s) 4.14 (12H, q, J = 7.1 Hz), 4.06–4.13 (12H, m), 1.21 (8H, t, J = 7.0 Hz). ESI-MS: m/z [**5⊂2e** + 2OTf]$^{2+}$ calcd 1221.4011, found 1221.4041.

Preparation of complex [(Ru(terpy))$_2$(5⊂2e)][OTf]$_8$. To a solution of [**5⊂2e**][OTf]$_4$ (0.030 g, 0.0109 mmol) dissolved in 1 : 1 EtOH–H_2O solution was added solid [$RuCl_3$(terpy)] (0.010 g, 0.020 mmol) and the mixture was brought to reflux for 24 h to give a deep red solution. The reaction mixture was cooled to room temperature and filtered through a Celite pad and washed with EtOH until the eluent was colourless. The filtrate was then reduced to half the volume and the addition of NaOTf produced a red precipitate. The red solid was dissolved in CH_3CN and isopropyl ether slowly diffused into the solution give a red solid in quantitative yield. ^{1}H NMR (500 MHz, CD_3CN): δ 9.43 (4H, d, J = 6.4 Hz), 9.11 (4H, d, J = 6.4 Hz), 8.83 (4H, s), 8.77 (4H, d, J = 8.1 Hz), 8.59 (4H, d, J = 8.1 Hz), 8.51 (4H, d, J = 8.1 Hz), 8.43 (4H, m), 8.42 (4H, m), 8.41 (4H, m), 8.09 (4H, d, J = 8.1 Hz), 7.93 (4H, m), 7.92 (4H, m), 7.91 (8H, m), 7.69 (4H, d, J = 8.1 Hz), 7.45 (4H, d, J = 5.2 Hz), 7.37 (4H, m, J = 5.3 Hz), 7.19 (4H, dd, J = 6.4, 6.3 Hz), 7.18 (4H, dd, J = 6.4, 6.3 Hz), 7.03 (4H, d, J = 8.7 Hz), 6.92 (4H, s), 5.87 (4H, s), 5.67 (4H, m), 4.81 (8H, s), 4.13–4.06 (12H, m), 4.13–4.06 (24H, m), 1.21 (8H, t, J = 7.0 Hz). UV-vis: λ_{max} = 486 nm. ESI-MS: m/z [(Ru(terpy))$_2$(**5⊂2e**) + 4OTf]$^{4+}$ calcd 852.6761, found 852.6795.

Preparation of MORF [Cd(H$_2$O)$_2$(3b⊂2d)(3b)][BF$_4$]$_6$. To a solution of **3b**[BF_4]$_2$, (13 mg, 0.025 mmol) in $MeNO_2$ (1 mL) was added 2 equivalents of **2d** (42 mg, 0.048 mmol). The resulting solution was stirred at room temperature for 1 h at which time [Cd(H$_2$O)$_6$][BF_4]$_2$ (5 mg, 13 mmol) dissolved in $MeNO_2$–MeOH (0.5 mL) was added. Slow diffusion of isopropyl ether into the $MeNO_2$ produced yellow crystals. Yield ~40%; determined to be a homogeneous sample by optical microscopy and identified as having formula {[Cd(H$_2$O)$_2$(**3b⊂2d**)(**3b**)][BF_4]$_6$·($MeNO_2$)$_{23}$} by single-crystal X-ray crystallography.

Single-crystal X-ray structure determinations. Crystals were mounted on a short glass fibre attached to a tapered copper pin. A full hemisphere of data were collected with 30 second frames on a Brüker APEX diffractometer fitted with a CCD based detector using MoK_α radiation (0.71073 Å). Decay (<1%) was monitored by 50 standard data frames measured at the beginning and end of data collections. Diffraction data and unit-cell parameters were consistent with the assigned space groups. Lorentzian polarization corrections and empirical absorption corrections, based on redundant data at varying effective azimuthal angles, were applied to the data set. The structure was solved by direct methods, completed by subsequent Fourier syntheses and refined with full-matrix least-squares methods against $|F^2|$ data. All non-hydrogen atoms were refined anisotropically. All hydrogen atoms were treated as idealized contributions. Scattering factors and anomalous dispersion coefficients are contained in the SHELXTL 5.03 program library.[22] All X-ray crystal structure graphics were created using the program DIAMOND.[23] A summary of crystal data collection, solution and structure refinement parameters are listed in Table 4. Details of the X-ray structure solutions can be found in the CIF format files deposited with the CCDC (numbers are listed in Table 4)†. This includes any problems with crystal quality, data collection or solution refinement that resulted in high residuals, as well as a description of any restraints necessary to attain the chemically reasonable models shown.

Acknowledgements

The authors thank NSERC of Canada for providing funds in the form of a Discovery Grant to S. J. L.

Notes and references

1 For reviews discussing pseudorotaxanes see: (*a*) T. B. Gasa, C. Valente and J. F. Stoddart, *Chem. Soc. Rev.*, 2011, **40**, 57; (*b*) M. Zhang, K. Zhu and F. Huang, *Chem. Commun.*, 2010, **46**, 8131; (*c*) A. Harada, A. Hashidzume, H. Yamaguchi and Y. Takashima, *Chem. Rev.*, 2009, **109**, 5974; (*d*) S. K. Kim and J. L. Sessler, *Chem. Soc. Rev.*, 2010, **39**, 3784; (*e*) V. Balzani, G. Bergamini and P. Ceroni, *Coord. Chem. Rev.*, 2008, **252**, 2456; (*f*) M. D. Lankshear and P. D. Beer, *Acc. Chem. Res.*, 2007, **40**, 657; (*g*) K. Kim, *Chem. Soc. Rev.*, 2002, **31**, 96; (*h*) V. Balzani, A. Credi, F. M. Raymo and J. F. Stoddart, *Angew. Chem., Int. Ed.*, 2000, **39**, 3348; (*i*) H. W. Gibson, in *Large Ring Molecules*, ed. J. A. Semlyen, John Wiley & Sons, New York, 1996, Ch. 6, p. 191; (*j*) F. M. Raymo and J. F. Stoddart, *Chem. Rev.*, 1999, **99**, 1643.

2 For some examples of [2]pseudorotaxanes formed with **DB248** see: (*a*) M. Klipfel, C. Rethore, T. Muller, S. Braese and W. Klopper, *Comput. Theor. Chem.*, 2011, **966**, 186; (*b*) C. Johnsen, P. C. Stein, K. A. Nielsen, A. D. Bond and J. O. Jeppesen, *Eur. J. Org. Chem.*, 2011, 759; (*c*) H. V. Huynh, W. Sim and C. F. Chin, *Dalton Trans.*, 2011, **40**, 11690; (*d*) H. W. Gibson, J. W. Jones, L. N. Zakharov, A. L. Rheingold and C. Slebodnick, *Chem.–Eur. J.*, 2011, **17**, 3192; (*e*) Y. Tokunaga, N. Wakamatsu, N. Ohiwa, O. Kimizuka, A. Ohbayashi, K. Akasaka, S. Saeki, K. Hisada, T. Goda and Y. Shimomura, *J. Org. Chem.*, 2010, **75**, 4950; (*f*) Y. Suzaki, A. Takagi and K. Osakada, *Chem. Lett.*, 2010, **39**, 510; (*g*) M. Lee, Z. Niu, D. V. Schoonover, C. Slebodnick and H. W. Gibson, *Tetrahedron*, 2010, **66**, 7077; (*h*) J.-L. Ko, S.-H. Ueng, C.-W. Chiu, C.-C. Lai, Y.-H. Liu, S.-M. Peng and S.-H. Chiu, *Chem.–Eur. J.*, 2010, **16**, 6950; (*i*) M. A. Bolla, J. Tiburcio and S. J. Loeb, *Tetrahedron*, 2008, **64**, 8423; (*j*) Y. Liu, C.-J. Li, H.-Y. Zhang, L.-H. Wang and X.-Y. Li, *Eur. J. Org. Chem.*, 2007, 4510; (*k*) D. Castillo, P. Astudillo, J. Mares, F. J. Gonzalez, A. Vela and J. Tiburcio, *Org. Biomol. Chem.*, 2007, **5**, 2252. For an excellent historical overview on secondary ammonium containing pseudorotaxanes see (*l*) P. R. Ashton, E. J. T. Chrystal, P. T. Glink, S. Menzer, C. Schiavo, N. Spencer, J. F. Stoddart, P. A. Tasker, A. J. P. White and D. J. Williams, *Chem.–Eur. J.*, 1996, **2**, 709 and references therein.

3 (*a*) Y. Tokunaga, T. Iwamoto, S. Nakashima, E.-I. Shoji and R. Nakata, *Tetrahedron Lett.*, 2011, **52**, 240; (*b*) S. Shinoda, T. Maeda, H. Miyake and H. Tsukube, *Supramol. Chem.*, 2011, **23**, 244; (*c*) D. J. Mercer, S. J. Vella, L. Guertin, N. D. Suhan, J. Tiburcio, V. N. Vukotic, J. A. Wisner and S. J. Loeb, *Eur. J. Org. Chem.*, 2011, 1763; (*d*) Y. Tokunaga, S. Nakashima, T. Iwamoto, K. Gambayashi, K. Hisada and T. Hoshi, *Heterocycles*, 2010, **80**, 819; (*e*) P. G. Clark, E. N. Guidry, W. Y. Chan, W. E. Steinmetz and R. H. Grubbs, *J. Am. Chem. Soc.*, 2010, **132**, 3405; (*f*) S. Sharma, G. J. E. Davidson and S. J. Loeb, *Chem. Commun.*, 2008, 582; (*g*) S. J. Loeb, J. Tiburcio, S. J. Vella and J. A. Wisner, *Org. Biomol. Chem.*, 2006, **4**, 667; (*h*) G. J. E. Davidson, S. J. Loeb, P. Passaniti, S. Silvi and A. Credi, *Chem.–Eur. J.*, 2006, **12**, 3233; (*i*) V. Melnig, A. Farcas, G. Rusu and C. Baban, *J. Optoelectron. Adv. Mater.*, 2005, **7**, 2875–2880; (*j*) S. J. Loeb, J. Tiburcio and S. J. Vella, *Org. Lett.*, 2005, **7**, 4923; (*k*) N. Georges, S. J. Loeb, J. Tiburcio and J. A. Wisner, *Org. Biomol. Chem.*, 2004, **2**, 2751; (*l*) G. J. E. Davidson and S. J. Loeb, *Dalton Trans.*, 2003, 4319; (*m*) P. R. Ashton, R. A. Bartsch,

Downloaded by University of California - San Diego on 01 September 2012
Published on 14 May 2012 on http://pubs.rsc.org | doi:10.1039/C2OB25200G

S. J. Cantrill, R. E. Hanes, Jr., S. K. Hickingbottom, J. N. Lowe, J. A. Preece, J. F. Stoddart, V. S. Talanov and Z.-H. Wang, *Tetrahedron Lett.*, 1999, **40**, 3661–3664; (*n*) S. J. Loeb and J. A. Wisner, *Angew. Chem., Int. Ed.*, 1998, **37**, 2838.

4 (*a*) Y. Tokunaga, T. Goda, N. Wakamatsu, R. Nakata and Y. Shimomura, *Heterocycles*, 2006, **68**, 5; (*b*) A. L. Hubbard, G. J. E. Davidson, R. H. Patel, J. A. Wisner and S. J. Loeb, *Chem. Commun.*, 2004, 138; (*c*) T. Clifford, A. Abushamleh and D. H. Busch, *Proc. Natl. Acad. Sci. U. S. A.*, 2002, **99**, 4830; (*d*) D. N. Reinhoudt, *J. Coord. Chem.*, 1988, **18**, 21.

5 G. J. E. Davidson, S. Sharma and S. J. Loeb, *Angew. Chem., Int. Ed.*, 2010, **49**, 4938.

6 (*a*) M. Suresh, A. K. Mandal, M. K. Kesharwani, N. N. Adarsh, B. Ganguly, R. K. Kanaparthi, A. Samanta and A. Das, *J. Org. Chem.*, 2011, **76**, 138; (*b*) S. J. Loeb, J. Tiburcio and S. J. Vella, *Chem. Commun.*, 2006, 1598.

7 W. Yang, Y. Li, J. Zhang, N. Chen, S. Chen, H. Liu and Y. Li, *J. Org. Chem.*, 2011, **76**, 7750.

8 (*a*) P. R. Ashton, I. Baxter, S. J. Cantrill, M. C. T. Fyfe, P. T. Glink, J. F. Stoddart, A. J. P. White and D. J. Williams, *Angew. Chem., Int. Ed.*, 1998, **37**, 1294; (*b*) D. A. Tramontozzi and S. J. Loeb, *Org. Biomol. Chem.*, 2005, **3**, 1393; (*c*) A. Ossenbach, H. Ruegger, A. Zhang, K. Fischer, A. Dieter Schluter and M. Schmidt, *Macromolecules*, 2009, **42**, 8781; (*d*) J. J. Pak, J. L. Mayo and E. Shurdha, *Tetrahedron Lett.*, 2006, **47**, 233.

9 (*a*) H. W. Gibson, H. Wang, K. Bonrad, J. W. Jones, C. Slebodnick, L. N. Zackharov, A. L. Rheingold, B. Habenicht, P. Lobue and A. E. Ratliff, *Org. Biomol. Chem.*, 2005, **3**, 2114; (*b*) T. Sato and T. Takata, *Tetrahedron Lett.*, 2007, **48**, 2797; (*c*) H. W. Gibson, H. Wang, C. Slebodnick, J. Merola, W. S. Kassel and A. L. Rheingold, *J. Org. Chem.*, 2007, **72**, 3381; (*d*) D. J. Hoffart, J. Tiburcio, A. de la Torre, L. K. Knight and S. J. Loeb, *Angew. Chem., Int. Ed.*, 2008, **47**, 97; (*e*) Y. Liu, C-J. Li, H-Y. Zhang, L-H. Wang, Q. Luo and G. Wang, *J. Chem. Phys.*, 2007, **126**, 064705.

10 For an example of direct tetra-bromination of **DB24C8** see: (*a*) M. Kallera, P. Staffeldb, R. Hauga, W. Freya, F. Giesselmannb and S. Laschata, *Liq. Cryst.*, 2011, **38**, 531. For a recent example of the direct tetra-nitration of **DB24C8** see: (*b*) S. J. Langford, M. J. Latter, V.-L. Lau, L. L. Martin and A. Mechler, *Org. Lett.*, 2006, **8**, 1372. For an example of direct tetra-iodination of **DB24C8** followed by complete replacement of iodine by methoxy see: (*c*) N. D. Suhan, L. Allen, M. T. Gharib, E. Viljoen, S. J. Vella and S. J. Loeb, *Chem. Commun.*, 2011, **47**, 5991.

11 S. J. Loeb, *Chem. Commun.*, 2005, 1511.

12 (*a*) S. Shrestha, C. Gimbert-Surinach, M. Bhadbhade and S. B. Colbran, *Eur. J. Inorg. Chem.*, 2011, 4331; (*b*) Y. Nakamura, A. Asami, T. Ogawa, S. Inokuma and J. Nishimura, *J. Am. Chem. Soc.*, 2002, **124**, 4329; (*c*) E. Luboch, A. Cygan and J. F. Biernat, *Tetrahedron*, 1990, **46**, 2461; (*d*) A. Cygan, J. F. Biernat and H. Chadzynsky, *Pol. J. Chem.*, 1979, **53**, 929.

13 I. R. Hanson, D. L. Hughes and M. R. Truter, *J. Chem. Soc., Perkin Trans. 2*, 1976, 972.

14 S. J. Vella, J. Tiburcio, J. W. Gauld and S. J. Loeb, *Org. Lett.*, 2006, **8**, 3421.

15 (*a*) S. J. Loeb and J. A. Wisner, *Chem. Commun.*, 1998, 2757; (*b*) S. J. Loeb and J. A. Wisner, *Chem. Commun.*, 2000, 845; (*c*) S. J. Loeb and J. A. Wisner, *Chem. Commun.*, 2000, 1939.

16 (*a*) S. J. Loeb, *Chem. Soc. Rev.*, 2007, **36**, 226; (*b*) S. J. Loeb, *Org. Nanostruct.*, 2008, 33; (*c*) D. J. Mercer and S. J. Loeb, *Dalton Trans.*, 2011, **40**, 6385.

17 (*a*) G. J. E. Davidson and S. J. Loeb, *Angew. Chem., Int. Ed.*, 2003, **42**, 74; (*b*) D. J. Hoffart and S. J. Loeb, *Angew. Chem., Int. Ed.*, 2005, **44**, 901; (*c*) D. J. Hoffart and S. J. Loeb, *Supramol. Chem.*, 2007, **19**, 89; (*d*) L. K. Knight, V. N. Vukotic, E. Viljoen, C. B. Caputo and S. J. Loeb, *Chem. Commun.*, 2009, 5585; (*e*) V. N. Vukotic and S. J. Loeb, *Chem.–Eur. J.*, 2010, **16**, 13630; (*f*) D. J. Mercer, V. N. Vukotic and S. J. Loeb, *Chem. Commun.*, 2011, **47**, 896.

18 (*a*) K. Chichak, M. C. Walsh and N. R. Branda, *Chem. Commun.*, 2000, 847; (*b*) G. J. E. Davidson, S. J. Loeb, N. A. Parekh and J. A. Wisner, *J. Chem. Soc., Dalton Trans.*, 2001, 3135.

19 Y. Suzaki, T. Taira, K. Osakada and M. Horie, *Dalton Trans.*, 2008, 4823 and references therein.

20 B. P. Sullivan, J. M. Calvert and T. J. Meyer, *Inorg. Chem.*, 1980, **19**, 1404.

21 J. P. Collin, S. Guillerez, J. P. Sauvage, F. Barigelletti, L. De Cola, L. Flamigni and V. Balzani, *Inorg. Chem.*, 1991, **30**, 4230.

22 G. M. Sheldrick, *Acta Crystallogr.*, 2008, **A64**, 112.

23 *DIAMOND 3.2, CRYSTAL IMPACT, Postfach 1251, D-53002*, Bonn, Germany, 2009.

 This journal is © The Royal Society of Chemistry 2012